

# Reduction of the spin susceptibility in the superconducting state of $\text{Sr}_2\text{RuO}_4$ observed by polarized neutron scattering

A. N. Petsch,<sup>1,\*</sup> M. Zhu,<sup>1</sup> Mechthild Enderle,<sup>2</sup> Z. Q. Mao,<sup>3,4</sup> Y. Maeno,<sup>3</sup> I. I. Mazin,<sup>5</sup> and S. M. Hayden<sup>1,†</sup>

<sup>1</sup>*H.H. Wills Physics Laboratory, University of Bristol, Bristol BS8 1TL, United Kingdom*

<sup>2</sup>*Institut Laue-Langevin, CS 20156, 38042 Grenoble Cedex 9, France*

<sup>3</sup>*Department of Physics, Graduate School of Science, Kyoto University, Kyoto 606-8502, Japan*

<sup>4</sup>*Department of Physics, Pennsylvania State University, University Park, Pennsylvania 16802, USA*

<sup>5</sup>*Department of Physics and Astronomy, George Mason University and  
Quantum Science and Engineering Center, Fairfax, VA 22030, USA*

(Dated: February 4, 2022)

Recent observations [A. Pustogow *et al.* Nature **574**, 72 (2019)] of a drop of the  $^{17}\text{O}$  nuclear magnetic resonance (NMR) Knight shift in the superconducting state of  $\text{Sr}_2\text{RuO}_4$  challenged the popular picture of a chiral odd-parity paired state in this compound. Here we use polarized neutron scattering (PNS) to show that there is a  $34 \pm 6\%$  drop in the magnetic susceptibility at the Ru site below the superconducting transition temperature. We measure at lower fields  $H \sim \frac{1}{3}H_{c2}$  than a previous PNS study allowing the suppression to be observed. The PNS measurements show a smaller susceptibility suppression than NMR measurements performed at similar field and temperature. Our results rule out the chiral odd-parity  $\mathbf{d} = \hat{\mathbf{z}}(k_x \pm ik_y)$  state and are consistent with several recent proposals for the order parameter including even-parity  $B_{1g}$  and odd-parity helical states.

*Introduction.*— $\text{Sr}_2\text{RuO}_4$  is a moderately correlated oxide metal which, which forms a good Fermi liquid and superconducts [1] below 1.5 K. It has been initially proposed as a solid state analogue [2, 3] of superfluid  $^3\text{He-A}$ , driven by proximity to ferromagnetism. The superconducting state was widely assumed to possess chiral odd-parity order [4, 5] with broken time-reversal symmetry [6]. An important property of odd-parity (triplet-paired) superconductors is that for some magnetic field directions the spin susceptibility may show no change upon entering the superconducting state. This property may be investigated by probes not sensitive to the superconducting diamagnetic screening currents, such as nuclear magnetic resonance (NMR) or polarized neutron scattering (PNS). Early studies of the susceptibility using the NMR Knight shift with  $^{17}\text{O}$  (NMR) [7] and PNS [8] detected no change while crossing the superconducting transition when magnetic fields were applied parallel to the  $\text{RuO}_2$ -planes or  $ab$ -planes. These observations supported the picture of triplet-pairing with an out-of-plane  $\mathbf{d}$ -vector or an unpinned in-plane  $\mathbf{d}$ -vector  $\perp \mathbf{H}$ . A muon-spin rotation ( $\mu\text{SR}$ ) study [6] observed that magnetic moments appeared below the superconducting transition temperature  $T_c$ . This was interpreted as evidence for time-reversal symmetry breaking (TRSB) in the superconducting phase. Further evidence for TRSB came from the detection of a Kerr effect [9] associated with the superconducting transition.

More recently, it has become clear that it is difficult to consistently describe the physical properties of the superconducting state with a simple odd-parity representation [10]. For example, the favored  $\mathbf{d} = \hat{\mathbf{z}}(k_x \pm ik_y)$  state implies the existence of edge currents which are not detected experimentally [11–14] and  $H_{c2}$  is much lower than expected [10]. Also an NMR experiment failed to

detect any changes in susceptibility for a  $c$ -axis field [15], even though it would have to be reduced below  $T_c$  in the  $\hat{\mathbf{z}}(k_x \pm ik_y)$  state. It was shown that rotation of the order parameter vector would be forbidden by the strong spin-orbit coupling [16, 17], which led one of us to conclude that “the Knight shift in  $\text{Sr}_2\text{RuO}_4$  remains a challenge for theorists; until this puzzle is resolved, we cannot use the Knight shift argument” [16].

Further progress has been made recently with a  $^{17}\text{O}$ -NMR study by Pustogow *et al.* [18] which detected a significant reduction in the Knight shift on entering the superconducting state for in-plane fields for the first time. This result has now been reproduced by Ishida *et al.* [19]. The observed reduction in the Knight shift on entering the superconducting state of  $\text{Sr}_2\text{RuO}_4$  shows that the spin susceptibility is reduced. This should also be observed in polarized neutron scattering measurements. However, a PNS study [8] with relatively poor statistics and at a field  $\mu_0 H = 1$  T was unable to observe a reduction.

In this paper, we report PNS measurements at a lower field ( $\mu_0 H = 0.5$  T) and with better statistics. We find a  $34 \pm 6\%$  drop in the magnetic susceptibility at the Ru site below the superconducting transition temperature. This is somewhat smaller than the  $63 \pm 8\%$  drop observed by NMR Knight shift measurements [19] at the in-plane oxygen site for a similar field  $\mu_0 H = 0.48$  T. We discuss possible reasons for the difference between the two observations and the constraints our results place on the allowed order superconducting order parameter.

*The spin susceptibility as a probe of the superconducting state.*—The transition to a superconducting state involves the pairing of electrons and hence a change to the spin wavefunction. In the case of singlet pairing where the spin susceptibility is suppressed everywhere (barring

state	basis function	line nodes	TRSB	$\chi_0(H, T \rightarrow 0)/\chi_0(n)$ with $\mathbf{H} \parallel$			state	basis function	line nodes	TRSB	$\chi_0(H, T \rightarrow 0)/\chi_0(n)$ with $\mathbf{H} \parallel$		
	$\Delta(\mathbf{k})$			[100]	[110]	[001]		$\mathbf{d}(\mathbf{k})$			[100]	[110]	[001]
$A_{1g}$	$k_x^2 + k_y^2$		X	0	0	0	$A_{1u}$	$\hat{x}k_x + \hat{y}k_y$		X	1/2	1/2	1
$A_{2g}$	$k_x k_y (k_x^2 - k_y^2)$	(v)	X	0	0	0	$A_{2u}$	$\hat{z}k_z$	(h)	X	1	1	0
$B_{1g}$	$k_x^2 - k_y^2$	(v)	X	0	0	0	$A_{2u}$	$\hat{x}k_y - \hat{y}k_x$	(v,h)	X	1/2	1/2	1
$B_{2g}$	$k_x k_y$	(v)	X	0	0	0	$A_{2u}$	$\hat{z}k_x k_y k_z (k_x^2 - k_y^2)$	(v,h)	X	1	1	0
$E_g(a)$	$k_x k_z; k_y k_z$	(v,h)	X	0	0	0	$B_{1u}$	$\hat{x}k_x - \hat{y}k_y$	(v,h)	X	1/2	1/2	1
$E_g(b)$	$(k_x \pm k_y)k_z$	(v,h)	X	0	0	0	$B_{1u}$	$\hat{z}k_x k_y k_z$	(v,h)	X	1	1	0
$E_g(c)$	$(k_x \pm i k_y)k_z$	(h)	✓	0	0	0	$B_{2u}$	$\hat{x}k_y + \hat{y}k_x$	(v,h)	X	1/2	1/2	1
							$B_{2u}$	$\hat{z}k_z (k_x^2 - k_y^2)$	(v,h)	X	1	1	0
							$E_u(a)$	$\hat{x}k_z; \hat{y}k_z$	(h)	X	0; 1	1/2	1
							$E_u(a)$	$\hat{z}k_x; \hat{z}k_y$	(v)	X	1	1	0
							$E_u(b)$	$(\hat{x} \pm \hat{y})k_z$	(h)	X	1/2	0; 1	1
							$E_u(b)$	$\hat{z}(k_x \pm k_y)$	(v)	X	1	1	0
							$E_u(c)$	$(\hat{x} \pm i\hat{y})k_z$	(h)	✓	1/2	1/2	1
							$E_u(c)$	$\hat{z}(k_x \pm i k_y)$		✓	1	1	0

TABLE I. Irreducible representations of superconducting order parameters compatible with the tetragonal point group  $D_{4h}$  with strong spin-orbit coupling [20]. The left and right panels are even-parity (singlet) and odd-parity (triplet) states, respectively. Column three and ten show whether states have vertical line nodes,  $\parallel k_z$ , (v), or horizontal line nodes,  $\perp k_z$  (h) on a 2D Fermi surface. States with  $k_\mu$  transform like  $\sin k_\mu$  while states with  $k_\mu^2$  transform like  $\cos k_\mu$ . Ticks indicate whether TRSB is present.  $\chi_0$  is calculated from Eqn. 2 in the  $H \rightarrow 0, T \rightarrow 0$  limit, for a cylindrical Fermi surface.

exotic cases as Ising superconductivity) its temperature dependence is described by the Yosida function [21, 22]. A triplet superconductor is described by a spinor order parameter,

$$\mathbf{\Delta} = \begin{bmatrix} \Delta_{\uparrow\uparrow} & \Delta_{\uparrow\downarrow} \\ \Delta_{\downarrow\uparrow} & \Delta_{\downarrow\downarrow} \end{bmatrix} = \Delta \begin{bmatrix} -d_x + id_y & d_z \\ d_z & d_x + id_y \end{bmatrix}, \quad (1)$$

where the  $\mathbf{d}$ -vector is  $\mathbf{d} = (d_x, d_y, d_z)$ . The non-interacting spin susceptibility tensor is given by [23]

$$\frac{\chi_{0,\alpha\beta}}{\chi_0(n)} = \delta_{\alpha\beta} + \int \frac{d\Omega}{4\pi} [Y(\hat{\mathbf{k}}, T) - 1] \Re \left\{ \frac{d_\alpha^*(\mathbf{k}) d_\beta(\mathbf{k})}{\mathbf{d}^*(\mathbf{k}) \cdot \mathbf{d}(\mathbf{k})} \right\}, \quad (2)$$

where the integral is over the Fermi surface,  $Y(\hat{\mathbf{k}}, T)$  is the Yosida function and  $\chi_0(n)$  the normal-state spin susceptibility. Table I shows  $\chi_0(T \rightarrow 0, H \rightarrow 0) = \chi_0(0)$  evaluated using Eqn. 2 for selected irreducible representations and applied field directions.

The measurements of the spin susceptibility in the superconducting state are complicated by diamagnetic screening due to supercurrents which precludes quantitative measurements with standard techniques such as SQUID magnetometry. The NMR Knight shift and PNS have been used successfully to measure the spin susceptibility in the superconducting state. The Knight shift,  $K$ , originates from the hyperfine interaction between the nuclear moment and the magnetic field at the nuclear site produced by the electrons surrounding that site, which is only indirectly related to the total magnetization. For instance, core polarization and spin-dipole interaction do not contribute to the latter, but affect the Knight shift, while spin and orbital moments have different spatial distributions and therefore produce different contributions

to  $K$  with opposite signs in some cases [24, 25]. In contrast, PNS probes the total magnetization density  $M(\mathbf{r})$  in absolute units induced by an external magnetic field  $\mu_0 H$ . The orbital and spin magnetization are equally weighted and  $M(\mathbf{r})$  is averaged in space. In the normal state of  $\text{Sr}_2\text{RuO}_4$ , three bands cross the Fermi surface [26]. The partially filled Ru  $t_{2g}$  orbitals account for the majority of the density of states at the Fermi energy. Hence the majority of the spin susceptibility is associated with the Ru site probed by PNS.

In PNS, the spatially varying density  $M(\mathbf{r})$  is measured by diffraction. This technique was first applied to  $\text{V}_3\text{Si}$  by Shull and Wedgwood [27]. It has also been used to probe cuprate [28] and iron-based [29, 30] superconductors where singlet pairing has been observed. Early PNS measurements by Shull and Wedgwood [27] of the temperature dependence of the induced magnetization in  $\text{V}_3\text{Si}$  showed that the susceptibility only dropped to about  $\frac{1}{3}$  of its normal state value for applied fields of  $\approx 0.1H_{c2}$ . This residual susceptibility is due to the orbital susceptibility present in transition metals [31, 32]. Importantly, such cancellation effects work very differently in NMR and PNS, for instance, in V metal NMR shows no or a very small change [33, 34] in the Knight shift across  $T_c$ , because of nearly exact cancellation of the core polarization (an effect specific to NMR) and the Fermi-contact term.

NMR and PNS probe susceptibility of superconducting in the mixed state and typically in relatively high magnetic fields  $\sim 1$  T. It is well known that vortices create low-energy electronic states [35, 36]. In the mixed state of conventional superconductors the associated quasiparticle density of states  $\mathcal{N}_F^*(H) \propto \mathcal{N}_F^*(n)H/H_{c2}$

comes from low-energy localized states in the vortex cores [35], while in superconductors with lines of gap nodes  $\mathcal{N}_F^*(H) \propto \mathcal{N}_F^*(n)\sqrt{H/H_{c2}}$  comes from the vicinity of the gap nodes in the momentum space, and partially from outside the vortex cores [36]. The same states give rise to a linear heat capacity and also contribute to the spin susceptibility. For example, a linear field dependence of  $\chi = M/H$  has been observed [29] in the superconducting state of  $\text{Ba}(\text{Fe}_{1-x}\text{Co}_x)_2\text{As}_2$ .

*Experimental method.*—The experimental set up and crystal were the same as described in Duffy et al. [8]. A single crystal (C117) of  $\text{Sr}_2\text{RuO}_4$  with dimensions of  $1.5\text{ mm} \times 2\text{ mm} \times 5\text{ mm}$  was cut from a crystal grown by floating-zone method and glued with GE-varnish on a copper stage with [100] aligned vertically. The sample size was chosen so as not to saturate the detector. To ensure good thermal contact on the sample the copper stage was connected via two 1 mm diameter copper wires to the dilution refrigerator.  $T_c$  of this sample is 1.47 K and  $\mu_0 H_{c2}(100\text{ mK}) = 1.43\text{ T}$  for  $\mathbf{H} \parallel [110]$  [8, 41]. We used the three-axis spectrometer IN20 at the Institut Laue-Langevin, Grenoble [42]. A vertical magnetic field was applied perpendicular to the scattering plane along the [100] direction. Measurements of the nuclear Bragg reflections (002) and (011) verified that the field was within  $0.11^\circ$  of the [100] direction. The PNS experiments were performed in the superconducting state at the (011) Bragg reflection with  $\mu_0 H = 0.5\text{ T}$ . The beam was monochromatic with  $E = 63\text{ meV}$ . The spectrometer beam polarization was  $93.2 \pm 0.1\%$ , measured at the (011) reflection using a Heusler monochromator and analyzer. Detector counts were normalized either to time or by using a neutron counter placed in the incident beam. Both methods produced consistent results. The sample was field cooled and test measurements with polarization analysis were performed to check for depolarization from the vortex lattice. We measured the beam polarization at the (002) and (011) Bragg reflections for  $\mu_0 H = 0.5\text{ T}$ , no measurable difference between superconducting and normal states could be detected. Susceptibility measurements were performed with a polarized beam without the analyzer as in Duffy et al. [8].

Polarized neutron scattering experiments can directly probe the real-space magnetization density  $\mathbf{M}(\mathbf{r})$  in the unit cell, induced by a large magnetic field  $\mu_0 H$ . Further details of the method and theory are given in our previous studies [8, 29]. Due to the periodic crystal structure, the applied magnetic field induces a magnetization density with spatial Fourier components  $\mathbf{M}(\mathbf{G})$ , where  $\mathbf{G}$  are the reciprocal lattice vectors, and

$$\mathbf{M}(\mathbf{G}) = \int_{\text{unit cell}} \mathbf{M}(\mathbf{r}) \exp(i\mathbf{G} \cdot \mathbf{r}) d\mathbf{r}. \quad (3)$$

We measure the flipping ratio  $R$ , defined as the ratio of the cross-sections,  $I_+$ ,  $I_-$ , of polarized incident beams with neutrons parallel or anti-parallel to the

applied magnetic field. A detector insensitive to the scattered spin polarization and summing over the final spin states was used. Because the induced moment is small, the experiment is carried out in the limit  $(\gamma r_0/2\mu_B)M(\mathbf{G})/F_N(\mathbf{G}) \ll 1$ . In this limit [8], the flipping ratio is,

$$R = 1 - \frac{2\gamma r_0}{\mu_B} \frac{M(\mathbf{G})}{F_N(\mathbf{G})}, \quad (4)$$

where the nuclear structure factor  $F_N(\mathbf{G})$  is known from the crystal structure and  $\gamma r_0 = 5.36 \times 10^{-15}\text{ m}$ . For the (011) reflection we used  $F_N = 4.63 \times 10^{-15}\text{ m f.u.}^{-1}$ .

*Results.*—In the present experiment we apply magnetic fields along the [100] direction to allow comparison with NMR measurements [18, 19]. We first established the normal state susceptibility  $\chi(n)$  by making measurements at  $T = 1.5\text{ K}$  and  $\mu_0 H = 2.5\text{ T}$  as shown in Fig. 1(a). Our signal,  $1 - R$ , is proportional to the induced moment (Eq. 4) and our error bars are determined by the number of counts in  $I_\pm$  and hence the counting time. Thus, the 2.5 T measurement (closed diamond) provides the most accurate estimate of the normal state susceptibility, shown by the horizontal solid line. The data has been converted to  $\chi$  using Eqn. 4 [43]. A further measurement (closed circle) was performed in the superconducting state at  $T = 0.06\text{ K}$  and  $\mu_0 H = 0.5\text{ T}$  with a total counting time of 52 hours in order to obtain good statistics and a small error bar. The difference between  $\chi(n)$  and the  $\chi(T=0.06\text{ K}, \mu_0 H=0.5\text{ T})$  point demonstrates a clear drop in  $\chi$  of  $34 \pm 6\%$  on entering the superconducting state.

Fig. 1(b) shows PNS and NMR results presented as a function of magnetic field. It is notable that PNS yields a larger susceptibility in the superconducting state than what can be deduced from the  $^{17}\text{O}$  Knight shift [19]  $K$  at comparable field and temperature. Specifically, at  $\mu_0 H \simeq 0.5\text{ T}$  and  $T \simeq 60\text{ mT}$ , we have  $\chi(\text{PNS})/\chi(n) = 0.66 \pm 0.06$  and  $K(\text{NMR})/K(n) = 0.37 \pm 0.08$ . In the Supplementary Material [39], we show how the measured susceptibility  $\chi$  is corrected for Fermi liquid effects (Stoner enhancement) and the orbital contribution. The corrected non-interacting spin susceptibility  $\chi_0$ , which can be compared with theory, is shown in Fig. 1(c).

As discussed above, PNS and NMR probe the magnetization in different ways so there are reasons why the results may be different. For the (011) Bragg reflection, the PNS method measures  $M[\mathbf{G} = (011)] \approx M_{\text{Ru}} \times f_{\text{Ru}}(\mathbf{G}) + 1.04 \times M_{\text{O}(2)} \times f_{\text{O}}(\mathbf{G}) \approx M_{\text{Ru}} \times f_{\text{Ru}}(\mathbf{G})$ , where  $f$  is the magnetic form factor and  $M$  is the magnetic moment on a given site. Note that the O(1) oxygen sites [see Fig. 1(c)] do not contribute to the magnetic signal observed at this reflection. Further, the moment on the oxygen O(2) sites is known to be small from NMR Knight shift measurements [19] and DFT calculations [44, 45]. Thus, our measurement is essentially sensitive only to the Ru sites where most of the moment

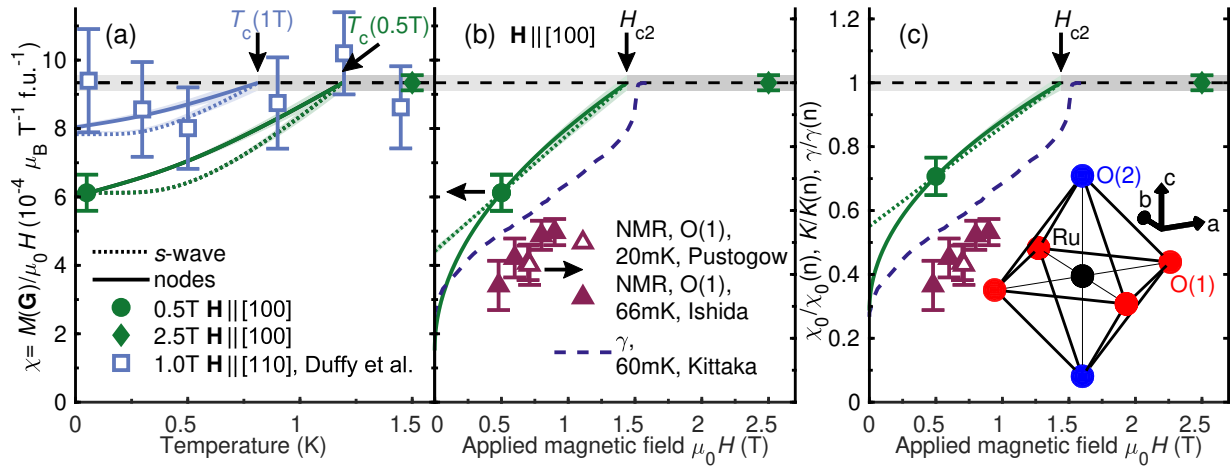


FIG. 1. PNS measurements of the susceptibility  $\chi = M(\mathbf{G})/\mu_0 H$  at  $\mathbf{G} = (011)$ . (a)  $T$ -dependence of  $\chi$  shows a drop below  $T_c$  for  $\mu_0 \mathbf{H} \parallel [100]$ . Results of Duffy et al. [8] with  $\mu_0 \mathbf{H} = 1 \text{ T} \parallel [110]$  (open symbols) are shown scaled by the Ru magnetic form factor [37].  $T$ -dependencies (dotted and solid lines) are calculated using the Yosida functions [21, 22, 38] and  $\chi(H)$  from (b). (b)  $H$ -dependence of  $\chi$  at  $T = 60 \text{ mK}$ .  $\chi(H)$  is fitted to simple  $s$ -wave and nodal models (see text). (c)  $H$ -dependence of the scaled non-interacting spin susceptibility  $\chi_0(H)/\chi_0(n)$  determined from (b) by correction for Stoner enhancement and orbital contribution [39]. Also shown are  $^{17}\text{O}$  NMR Knight shift,  $K$ , data at similar temperatures from Pustogow et al. [18] and Ishida et al. [19], and the measured linear coefficient of the specific heat,  $\gamma = C_e/T$  from Kittaka et al. [40]. Both quantities have been scaled to their normal state values.

resides. In contrast, recent NMR experiments [18, 19] probed the oxygen O(1) sites.

As mentioned,  $\chi_0(T)$  for an isotropic  $s$ -superconductor is expected to follow the Yosida function [21]. This function can be easily modified [22] to account for a superconductor with vertical line nodes. At low temperatures the drop in  $\chi \equiv M/H$  will be field-dependent due to the introduction of vortices by the magnetic field. Modeling the effect of vortices on the spin susceptibility is theoretically difficult; in addition,  $\text{Sr}_2\text{RuO}_4$  shows a first order phase transition at  $H_{c2}$  with a step in the spin magnetization [46–48]. Nevertheless, in Fig. 1(c) we fit two simple illustrative low-temperature field dependencies of  $\chi_0(H)$  with  $\chi_{0,s}(H) = \chi_0(0) + \Delta\chi H/H_{c2}$  and  $\chi_{0,nodal}(H) = \chi_0(0) + \Delta\chi \sqrt{H/H_{c2}}$  for the  $s$ -wave and nodal cases using the actual  $H_{c2}$  [35, 36]. Our  $s$ -wave and nodal field-dependent fits yield zero-field residual values of  $\chi_0(0)/\chi_0(n)$  of  $0.55 \pm 0.09$  and  $0.29 \pm 0.15$  respectively. Both fits give  $\chi \approx 8 \times 10^{-4} \mu_B T^{-1} \text{ f.u.}^{-1}$  for  $\mu_0 H = 1 \text{ T}$ .

Our data is consistent with two interesting scenarios as  $H \rightarrow 0$ : (i) a rapid reduction of  $\chi_0$  below  $\frac{1}{3}H_{c2}$  (solid line in Fig. 1(c)); (ii) a large residual contribution to  $\chi_0$  in the  $H \rightarrow 0$  limit (dotted line). Case (i) would be consistent with an even-parity (singlet) state with deep minima or nodes [36] in the gap and a small residual spin susceptibility. In case (ii) there would be a large residual spin susceptibility. This would be qualitatively consistent with various states in Table I and other proposals discussed below.

Both  $\chi_0(H)$  and the linear coefficient of specific heat  $\gamma(H) = C_e/T$  can detect the low-energy states intro-

duced by vortices. For a singlet superconductor, they are expected to show similar behavior [48]. In Fig. 1(b,c) we reproduce the measured [40]  $\gamma(H)$  for  $\mathbf{H} \parallel [100]$  and the recent NMR Knight shift [18, 19] which both yield smaller values when normalized to the normal state [39].

It is instructive to compare the present PNS data with that of Duffy et al. [8] measured with  $\mathbf{H} \parallel [110]$ . From Table I one can see that the effect of the field is expected to be the same for the [100] and [110] directions for all order parameter symmetries, except for two of the  $E_u$  states. In Fig. 1(a), we also show the PNS results of Duffy et al. [8] (open squares) measured at a field of 1 T with  $\mathbf{H} \parallel [110]$ . These were probed at the (002) Bragg peak and have therefore been scaled by the ratio of the Ru form factors [37, 49] at (011) and (002) for comparison. The solid and dotted lines show the expected  $T$ -dependence based on the fitted  $\chi(H)$  in Fig. 1(b,c) and the Yosida function [21, 22]. It is likely that Duffy et al. [8] were unable to resolve a change because of the lower statistical accuracy and use of a higher field, where the suppression effect is smaller due to the field induced density of states. However, the  $E_u$  state  $\mathbf{d} = (\hat{x} - \hat{y})k_z$  (which shows no change in  $\chi_0$  for  $\mathbf{H} \parallel [110]$  and a change for  $\mathbf{H} \parallel [100]$ ) cannot currently be ruled out by the PNS experiments.

*Discussion.*—Many superconducting states have been proposed for  $\text{Sr}_2\text{RuO}_4$ . Some of those are shown in Table I and, following the observations of Pustogow et al. [18], there have also been new theoretical proposals [50–52]. The PNS measurements reported here yield a non-interacting spin susceptibility in the superconducting state  $\chi_0(\mu_0 H = 0.5 \text{ T})/\chi_0(n) = 0.71 \pm 0.06$  which

is larger than the NMR Knight shift [18, 19]. Thus the PNS data better match different states. We concluded above that the residual  $\chi_0(0)/\chi_0(n) = 0.55 \pm 0.09$  or  $0.29 \pm 0.15$  for non-nodal [e.g.  $\hat{\mathbf{x}}k_x + \hat{\mathbf{y}}k_y$ ,  $\hat{\mathbf{z}}(k_x \pm ik_y)$ ] or (near) nodal [e.g.  $s'$ ,  $d_{x^2-y^2}$ ,  $(k_x \pm ik_y)k_z$ ] gaps respectively. Thus, our PNS measurements do not rule out all odd-parity states, but they do rule out those with  $\chi_0(0)/\chi_0(n) = 1$  in Table I. This includes the previously widely considered chiral  $p$ -wave  $\mathbf{d} = \hat{\mathbf{z}}(k_x \pm ik_y)$  state [2, 4, 5, 53]. Odd-parity states with in-plane  $\mathbf{d}$  vectors such as the helical triplet (e.g.  $\mathbf{d} = \hat{\mathbf{x}}k_x + \hat{\mathbf{y}}k_y$ ) states proposed by Rømer et al. [50] have a partial ( $\approx 50\%$ ) suppression of  $\chi_s$  and therefore are not ruled out. Other states that are qualitatively compatible with our observations include the TRSB  $s' + id_{x^2-y^2}$  and non-unitary  $\hat{\mathbf{x}}k_x \pm i\hat{\mathbf{y}}k_y$  states [50] proposed by Rømer et al. [50], states resulting from the 3D model of Røising et al. [51], the TRSB  $d_{xz \pm iyz}$  of Zutic and Mazin [16, 54], or the newest  $d + ig$  proposal by Kivelson et al. [52].

The smaller  $\chi_0(0)/\chi_0(n) = 0.29 \pm 0.15$  for nodal states is compatible with even-parity order parameters with deep minima or nodes in the gap, listed above. Particularly, if other (impurity or orbital) contributions are included in our estimated  $\chi_0$  which are not due to quasi-particles excitations [39, 55, 56]. The nodal  $s'$ -wave and  $d_{x^2-y^2}$ -wave states are supported by thermal conductivity [57], angle-dependent specific heat [40], penetration depth [58] and quasiparticle interference experiments [59], albeit not by the evidence of TRSB, or by the recently observed discontinuity in the  $c_{66}$  shear modulus [60]. Future polarized neutron scattering measurements at lower fields and other field directions will place further constraints on the allowed paired states.

The authors are grateful for helpful discussions with J. F. Annett, S. E. Brown, K. Ishida, A. T. Rømer, and S. Yonezawa. Work is supported by EPSRC Grant EP/R011141/1, the Centre for Doctoral Training in Condensed Matter Physics (EPSRC Grant EP/L015544/1), JSPS Kakenhi (Grants JP15H5852 and JP15K21717) and the JSPS-EPSRC Core-to-Core Program ‘‘Oxide-Superspin (OSS)’’.

\* a.petsch@bristol.ac.uk

† s.hayden@bristol.ac.uk

- [1] Y. Maeno, H. Hashimoto, K. Yoshida, S. Nishizaki, T. Fujita, J. G. Bednorz, and F. Lichtenberg, *Nature* **372**, 532 (1994).
- [2] T. M. Rice and M. Sigrist, *J Phys. : Condens Matter* **7**, L643 (1995).
- [3] I. I. Mazin and D. J. Singh, *Phys. Rev. Lett.* **79**, 733 (1997).
- [4] A. P. Mackenzie and Y. Maeno, *Rev. Mod. Phys.* **75**, 657 (2003).
- [5] Y. Maeno, S. Kittaka, T. Nomura, S. Yonezawa, and K. Ishida, *J. Phys. Soc. Japan* **81**, 011009 (2012).
- [6] G. M. Luke, Y. Fudamoto, K. M. Kojima, M. I. Larkin, J. Merrin, B. Nachumi, Y. J. Uemura, Y. Maeno, Z. Q. Mao, Y. Mori, H. Nakamura, and M. Sigrist, *Nature* **394**, 558 (1998).
- [7] K. Ishida, H. Mukuda, Y. Kitaoka, K. Asayama, Z. Q. Mao, Y. Mori, and Y. Maeno, *Nature* **396**, 658 (1998).
- [8] J. A. Duffy, S. M. Hayden, Y. Maeno, Z. Mao, J. Kulda, and G. J. McIntyre, *Phys. Rev. Lett.* **85**, 5412 (2000).
- [9] J. Xia, Y. Maeno, P. T. Beyersdorf, M. M. Fejer, and A. Kapitulnik, *Phys. Rev. Lett.* **97** (2006).
- [10] A. P. Mackenzie, T. Scaffidi, C. W. Hicks, and Y. Maeno, *npj Quant. Mater.* **2**, 40 (2017).
- [11] J. R. Kirtley, C. Kallin, C. W. Hicks, E.-A. Kim, Y. Liu, K. A. Moler, Y. Maeno, and K. D. Nelson, *Phys. Rev. B* **76**, 014526 (2007).
- [12] C. W. Hicks, J. R. Kirtley, T. M. Lippman, N. C. Koshnick, M. E. Huber, Y. Maeno, W. M. Yuhasz, M. B. Maple, and K. A. Moler, *Phys. Rev. B* **81**, 214501 (2010).
- [13] P. J. Curran, V. V. Khotkevych, S. J. Bending, A. S. Gibbs, S. L. Lee, and A. P. Mackenzie, *Phys. Rev. B* **84**, 104507 (2011).
- [14] P. J. Curran, S. J. Bending, W. M. Desoky, A. S. Gibbs, S. L. Lee, and A. P. Mackenzie, *Phys. Rev. B* **89**, 144504 (2014).
- [15] H. Murakawa, K. Ishida, K. Kitagawa, Z. Q. Mao, , and Y. Maeno, *Phys. Rev. Lett.* **93**, 167004 (2004).
- [16] I. Zutic and I. Mazin, *Phys. Rev. Lett.* **95**, 217004 (2005).
- [17] B. Kim, S. Khmelevskiy, I. I. Mazin, and D. F. A. . C. Franchini, *npj Quantum Materials* volume **2**, 37 (2017).
- [18] A. Pustogow, Y. Luo, A. Chronister, Y.-S. Su, D. A. Sokolov, F. Jerzembeck, A. P. Mackenzie, C. W. Hicks, N. Kikugawa, S. Raghu, E. D. Bauer, and S. E. Brown, *Nature* **574**, 72 (2019).
- [19] K. Ishida, M. Manago, K. Kinjo, and Y. Maeno, *J. Phys. Soc. Japan* **89**, 034712 (2020).
- [20] J. F. Annett, *Adv. Phys.* **39**, 83 (1990).
- [21] K. Yosida, *Phys. Rev* **110**, 769 (1958).
- [22] H. Won and K. Maki, *Phys. Rev. B* **49**, 1397 (1994).
- [23] A. J. Leggett, *Rev. Mod. Phys.* **47**, 331 (1975).
- [24] E. Pavarini and I. I. Mazin, *Phys. Rev. B* **74**, 035115 (2006).
- [25] Y. Luo, A. Pustogow, P. Guzman, A. P. Dioguardi, S. M. Thomas, F. Ronning, N. Kikugawa, D. A. Sokolov, F. Jerzembeck, A. P. Mackenzie, C. W. Hicks, E. D. Bauer, I. I. Mazin, and S. E. Brown, *Phys. Rev. X* **9**, 021044 (2019).
- [26] T. Oguchi, *Phys. Rev. B* **51**, 1385 (1995).
- [27] C. G. Shull and F. A. Wedgwood, *Phys. Rev. Lett.* **16**, 513 (1966).
- [28] J. Boucherle, J. Henry, R. J. Papoular, J. Rossat-Mignod, J. Schweizer, F. Tasset, and G. Uimin, *Physica B* **192**, 25 (1993).
- [29] C. Lester, J.-H. Chu, J. G. Analytis, A. Stunault, I. R. Fisher, and S. M. Hayden, *Phys. Rev. B* **84**, 134514 (2011).
- [30] J. Brand, A. Stunault, S. Wurmehl, L. Harnagea, B. Büchner, M. Meven, and M. Braden, *Phys. Rev. B* **89**, 045141 (2014).
- [31] A. M. Clogston, A. C. Gossard, V. Jaccarino, and Y. Yafet, *Phys. Rev. Lett.* **9**, 262 (1962).
- [32] R. M. White, *Quantum Theory of Magnetism* (Springer, Berlin, 1983).
- [33] R. J. Noer and W. D. Knight, *Rev. Mod. Phys.* **36**, 177 (1964).

- [34] I. Garifullin, N. Garifyanov, R. Salikhov, and L. Tagirov, *JETP Letters* **87**, 316 (2008).
- [35] C. Caroli, P. G. D. Gennes, and J. Matricon, *Phys. Lett.* **9**, 307 (1964).
- [36] G. E. Volovik, *JETP Lett.* **58**, 469 (1993).
- [37] P. J. Brown, *International Tables for Crystallography Vol. C* (Kluwer, Dordrecht, 1992) p. 391.
- [38] P. W. Anderson and P. Morel, *Phys. Rev.* **123**, 1911 (1961).
- [39] See Supplemental Material at [URL will be inserted by publisher] for a discussion of how the measured susceptibility  $\chi$  is corrected for interaction effects (Stoner enhancement or Fermi liquid correction) and the orbital susceptibility to yield the non-interacting spin susceptibility  $\chi_0$ . A two-fluid model for the susceptibility and electronic heat capacity is also discussed.
- [40] S. Kittaka, S. Nakamura, T. Sakakibara, N. Kikugawa, T. Terashima, S. Uji, D. A. Sokolov, A. P. Mackenzie, K. Irie, Y. Tsutsumi, K. Suzuki, and K. Machida, *J. Phys. Soc. Japan* **87**, 093703 (2018).
- [41] Z. Q. Mao, Y. Maeno, and H. Fukazawa, *Mater. Res. Bull.* **35**, 1813 (2000).
- [42] S. M. Hayden, M. Enderle, A. Petsch, and M. Zhu, “The Nature of the Superconducting State in  $\text{Sr}_2\text{RuO}_4$ ,” (2019).
- [43]  $M(\mathbf{G})$  includes the effect of the magnetic form factor. The spin-orbit interaction is negligible [61] and nuclear polarization [62] or ordering contributions have been neglected.
- [44] M. W. Haverkort, I. S. Elfimov, L. H. Tjeng, G. A. Sawatzky, and A. Damascelli, *Phys. Rev. Lett.* **101**, 026406 (2008).
- [45] C. Noce and M. Cuoco, *Phys. Rev. B* **59**, 2659 (1999).
- [46] K. Deguchi, M. A. Tanatar, Z. Mao, T. Ishiguro, and Y. Maeno, *J. Phys. Soc. Japan* **71**, 2839 (2002).
- [47] S. Kittaka, A. Kasahara, T. Sakakibara, D. Shibata, S. Yonezawa, Y. Maeno, K. Tenya, and K. Machida, *Phys. Rev. B* **90**, 220502 (2014).
- [48] Y. Amano, M. Ishihara, M. Ichioka, N. Nakai, and K. Machida, *Phys. Rev. B* **91**, 144513 (2015).
- [49] The available form factor  $\text{Ru}^+$  was used.
- [50] A. T. Rømer, D. D. Scherer, I. M. Eremin, P. J. Hirschfeld, and B. M. Andersen, *Phys. Rev. Lett.* **123**, 247001 (2019).
- [51] H. S. Røising, T. Scaffidi, F. Flicker, G. F. Lange, and S. H. Simon, *Phys. Rev. Research* **1**, 033108 (2019).
- [52] S. A. Kivelson, A. C. Yuan, B. J. Ramshaw, and R. Thomale, arXiv:2002.00016 (2020).
- [53] G. Baskaran, *Physica B* **223-224**, 490 (1996).
- [54] H. G. Suh, H. Menke, P. Brydon, C. Timm, A. Ramires, and D. F. Agterberg, arXiv:1912.09525 (2019).
- [55] A. A. Abrikosov and L. P. Gor’kov, *Soviet Phys. JETP* **15**, 752 (1962).
- [56] Y. Bang, *Phys. Rev. B* **85**, 104524 (2012).
- [57] E. Hassinger, P. Bourgeois-Hope, H. Taniguchi, S. René de Cotret, G. Grissonnanche, M. S. Anwar, Y. Maeno, N. Doiron-Leyraud, and L. Taillefer, *Phys. Rev. X* **7**, 011032 (2017).
- [58] I. Bonalde, B. D. Yanoff, M. B. Salamon, D. J. Van Harlingen, E. M. E. Chia, Z. Q. Mao, and Y. Maeno, *Phys. Rev. Lett.* **85**, 4775 (2000).
- [59] R. Sharma, S. D. Edkins, Z. Wang, A. Kostin, C. Sow, Y. Maeno, A. P. Mackenzie, J. C. S. Davis, and V. Madhavan, *Proc. Nat. Acad. Sci.* **117**, 5222 (2020).
- [60] S. Ghosh, A. Shekhter, F. Jerzembeck, N. Kikugawa, D. A. Sokolov, M. Brando, A. P. Mackenzie, C. W. Hicks, and B. J. Ramshaw, arXiv:2002.06130 (2020).
- [61] C. G. Shull, *Phys. Rev. Lett.* **10**, 297 (1963).
- [62] Y. Ito and C. G. Shull, *Phys. Rev.* **185**, 961 (1969).

## Supplementary Material: Orbital contributions to the susceptibility, Fermi liquid corrections and a two fluid model

Our polarized neutron scattering measurement probes the total magnetic moment (or associated susceptibility) including spin and orbital contributions. In addition, the spin susceptibility in  $\text{Sr}_2\text{RuO}_4$  is subject to an exchange or Stoner enhancement. The effect of the Stoner enhancement is temperature and field dependent. Here we describe how these two effects can be taken into account when comparison is made with theory.

### BACKGROUND

Theoretical models describing the spin susceptibility in superconductors such as  $\text{Sr}_2\text{RuO}_4$  typically aim to calculate the non-interacting susceptibility. In the normal state this would be  $\mu_B^2 \mathcal{N}_F$  and would be obtained from a density functional theory (DFT) band structure calculation, where the non-interacting unrenormalized electron density of states at the Fermi energy is  $\mathcal{N}_F$ . In Landau Fermi Liquid theory [1], the  $H \rightarrow 0$  non-interacting renormalized spin susceptibility  $\chi_0$  and specific heat coefficient  $\gamma = C_e/T$  are given by  $\chi_0 = \mu_B^2 \mathcal{N}_F^*$  and  $\gamma = (\pi^2/3) k_B^2 \mathcal{N}_F^*$ , where  $\mathcal{N}_F^*$  is the quasiparticle density of states.

Polarized neutron scattering measurements probe the total magnetic moment (or associated susceptibility) including spin and orbital contributions. In addition,  $\chi_0$  in  $\text{Sr}_2\text{RuO}_4$  is subject to a Stoner enhancement where the Stoner factor is  $I$ . Our experiments are performed in a magnetic field, where we define the susceptibility  $\chi_0(H) = M/\mu_0 H$  and  $\chi_0(n)$  denotes the normal state value (say at  $H_{c2}$ ).

The susceptibility due to the orbital and spin components is then given by

$$\chi(H) = \chi_{\text{orb}} + \chi_{\text{spin}}(H) = \chi_{\text{orb}} + \frac{\chi_0(H)}{1 - I\chi_0(H)}. \quad (1)$$

DFT calculations estimate  $\chi_{\text{orb}} \approx 1.5 \times 10^{-4} \mu_B \text{T}^{-1} \text{f.u.}^{-1}$ , although, DMFT suggests an enhancement by fluctuations of the orbital contribution up to a factor of two [2, 3] to  $\sim 3 \times 10^{-4} \mu_B \text{T}^{-1} \text{f.u.}^{-1}$ . It will be convenient to define the ratio of the orbital and spin parts of the susceptibility in the normal state  $f$  as

$$f = \frac{\chi_{\text{orb}}}{\chi_{\text{spin}}(n)} = \chi_{\text{orb}} \frac{1 - I\chi_0(n)}{\chi_0(n)}. \quad (2)$$

Based on the DFT calculations, we estimate  $f = 0.11$ .

We may use measured normal state values of the susceptibility and linear coefficient of the electronic specific heat  $\gamma$  to estimate Stoner enhancement. The measured susceptibility for fields parallel to the  $a$ -axis is  $\chi_a = 0.91 \text{ emu mole}^{-1} = 1.61 \times 10^{-3} \mu_B \text{T}^{-1} \text{f.u.}^{-1}$  [4]. From the measured susceptibility and the estimate of  $\chi_{\text{orb}}$  we obtain  $\chi_{\text{spin}}(n) = 1.46 \times 10^{-3} \mu_B \text{T}^{-1} \text{f.u.}^{-1} =$

$1.04 \times 10^{-8} \text{ mole}^{-1}$ . The linear specific heat is linear specific heat  $\gamma(n) = 40 \text{ mJ mole}^{-1} \text{K}^{-2}$ , yielding a Wilson ratio  $W = (\chi/\gamma) \times (\pi^2 k_B^2)/(3\mu_0 \mu_B^2) = 1.5$ . Assuming a Stoner enhancement factor equal to the Wilson ratio, the last term of Eq. 1 is

$$W = \frac{1}{1 - I\chi_0(n)}.$$

We can estimate  $I\chi_0(n) = S = 0.33$ . The enhancement of the spin susceptibility can also be understood through Fermi liquid theory ( $F_0^a$  parameter) [5]. In the case of  $^3\text{He}$ , which has  $W \approx 3$ , Fermi liquid effects are required to understand the temperature dependence of the spin susceptibility of the superfluid phases [6].

### CORRECTION FOR ORBITAL SUSCEPTIBILITY AND STONER ENHANCEMENT

In Fig.1 of the main paper we plot susceptibilities normalized to their normal state values as a function of field and temperature. We should remember that in the case of the polarized neutron scattering we measure  $M(\mathbf{G})/\mu_0 H$  in absolute units. This susceptibility contains a form factor due to the electron orbital hence the values are lower those quoted above by a factor of 0.68[7]. We define relative susceptibilities

$$X(H) = \chi(H)/\chi(n),$$

and

$$X_0(H) = \chi_0(H)/\chi_0(n),$$

where  $\chi(H)$  refers to the measured susceptibility in Eq. 1 and  $\chi_0(H)$  refers to the corresponding non-interacting spin susceptibility. Fig.1(a,b) shows the measured  $X(B, T)$ .  $X_0(H)$  and  $X(H)$  are related through the equations

$$X(H) = \frac{\chi_{\text{orb}} + \frac{\chi_0(H)}{1 - I\chi_0(H)}}{\chi_{\text{orb}} + \frac{\chi_0(n)}{1 - I\chi_0(n)}} \quad (3)$$

$$= \left( X_0(H) + \frac{f[1 - X_0(H)]}{(f+1)(1-S)} \right) \frac{1-S}{1 - SX_0(H)} \quad (4)$$

$$X_0(H) = \frac{f(X(H) - 1) + X(H)}{1 + (1+f)S(X-1)} \quad (5)$$

Thus we use Eqn. 5 with  $f = 0.11$  and  $S = 0.33$  to correct for orbital susceptibility and Stoner enhancement of the susceptibility and relate the data and curves in Fig. 1(b) and (c). In particular, as discussed in the main text, theory makes predictions for the field dependencies of the non-interacting spin susceptibility  $\chi_{0,s}(H) = \chi_0(0) + \Delta\chi_0 H/H_{c2}$  and  $\chi_{0,\text{nodal}}(H) = \chi_0(0) + \Delta\chi_0 \sqrt{H/H_{c2}}$ .

$X(H) = \chi(H)/\chi(n)$	$X(H)$	$X_0(H)$
$\chi(\mu_0 H = 0.5\text{T})$	0.66(6)	0.71(6)
$\chi(0), \chi_0(0)$ ( <i>s</i> -wave)	0.47(9)	0.55(9)
$\chi(0), \chi_0(0)$ (nodal)	0.16(14)	0.29(15)

TABLE I. Measured and corrected susceptibilities. The table shows the effect of the correction for the orbital susceptibility and Stoner enhancement (Fermi liquid effects) on the susceptibility in the superconducting state.

## TWO-FLUID MODEL FOR SPIN SUSCEPTIBILITY AND HEAT CAPACITY

As mentioned above, the linear coefficient of the electronic specific heat  $\gamma = C_e/T$  and the non-interacting spin susceptibility  $\chi_0$  should be proportional to the quasi-particle density of states  $\mathcal{N}_F^*$ . This would imply that  $\chi_0$  and  $\gamma$  are also proportional to each other and hence, the relative values  $\gamma(H)/\gamma(n)$  and  $X_0(H) = \chi_0(H)/\chi_0(n)$  should be equal. In Fig. 1(c) of the main paper the relative values  $\gamma(H)/\gamma(n)$  and  $\chi_0(H)/\chi_0(n)$  are shown, however, they display different field dependencies. This could be due to various causes (i-iv). (i) It could be that the orbital susceptibility in  $\text{Sr}_2\text{RuO}_4$  is larger than the applied value of  $1.5 \times 10^{-4} \mu_B \text{T}^{-1} \text{f.u.}^{-1}$  calculated by DFT and is instead closer to the fluctuation enhanced doubled value predicted by DMFT [2, 3]. (ii) The sample we probed by PNS has a larger residual  $\gamma$  than the sample used in the specific heat measurements reproduced in Fig. 1(b,c) in the main paper[8]. Sample dependence of the linear coefficient  $\gamma$  has been reported in  $\text{Sr}_2\text{RuO}_4$  in the past[8, 9]. (iii) There is a nuclear polarization of some of the Sr and Ru nuclei due to the applied field and low temperature, which would give an additional term in the PNS flipping ratio [10, 11]. (iv) The two-fluid model, which describes a superconductor as a superposition of a superconducting condensate and a normal Fermi-liquid with no interference, is not a sufficiently accurate description for the superconducting state in  $\text{Sr}_2\text{RuO}_4$ .

The measured  $^{17}\text{O}$  NMR Knight shifts reproduced in Fig. 1(b,c)[12, 13] in the main paper are as well as the spin susceptibility subject to Stoner enhancement and should also contain orbital contributions. If we assume the same Stoner factor ( $S=0.33$ ), that we observe that the relative non-interacting Knight shifts  $K_0(H)/K_0(n)$  analogue to  $X_0$  in Eq. 5 agrees with the reproduced relative linear coefficient of the electronic specific heat  $\gamma(H)/\gamma(n)$  without any orbital contribution ( $f = 0$ ).

- 
- [1] P. Coleman, *Introduction to Many-Body Physics* (Cambridge University Press, 2015).
  - [2] M. Kim, J. Mravlje, M. Ferrero, O. Parcollet, and A. Georges, *Phys. Rev. Lett.* **120**, 126401 (2018).
  - [3] A. Tamai, M. Zingl, E. Rozbicki, E. Cappelli, S. Riccò, A. de la Torre, S. M. Walker, F. Bruno, P. King, W. Meevasana, M. Shi, M. Radović, N. Plumb, A. Gibbs, A. Mackenzie, C. Berthod, H. Strand, M. Kim, A. Georges, and F. Baumberger, *Phys. Rev. X* **9** (2019).
  - [4] K. Ishida, H. Mukuda, Y. Kitaoka, K. Asayama, Z. Q. Mao, Y. Mori, and Y. Maeno, *Nature* **396**, 658 (1998).
  - [5] I. I. Mazin and R. E. Cohen, *Ferroelectrics* **164**, 263 (1997).
  - [6] A. J. Leggett, *Phys. Rev. Lett.* **14**, 536 (1965).
  - [7] P. J. Brown, *International Tables for Crystallography Vol. C* (Kluwer, Dordrecht, 1992) p. 391.
  - [8] S. Kittaka, S. Nakamura, T. Sakakibara, N. Kikugawa, T. Terashima, S. Uji, D. A. Sokolov, A. P. Mackenzie, K. Irie, Y. Tsutsumi, K. Suzuki, and K. Machida, *J. Phys. Soc. Japan* **87**, 093703 (2018).
  - [9] S. Nishizaki, Y. Maeno, and Z. Mao, *J. Phys. Soc. Jpn.* **69**, 572 (2000).
  - [10] C. G. Shull and R. P. Ferrier, *Phys. Rev. Lett.* **10**, 295 (1963).
  - [11] Y. Ito and C. G. Shull, *Phys. Rev.* **185**, 961 (1969).
  - [12] A. Pustogow, Y. Luo, A. Chronister, Y.-S. Su, D. A. Sokolov, F. Jerzembeck, A. P. Mackenzie, C. W. Hicks, N. Kikugawa, S. Raghu, E. D. Bauer, and S. E. Brown, *Nature* **574**, 72 (2019).
  - [13] K. Ishida, M. Manago, K. Kinjo, and Y. Maeno, *J. Phys. Soc. Japan* **89**, 034712 (2020).